Manipulation of vector beam polarization with geometric metasurfaces

Guo, Qinghua; Schlickriede, Christian; Wang, Dongyang; Liu, Hongchao; Xiang, Yuanjiang; Zentgraf, Thomas; Zhang, Shuang

DOI:
10.1364/OE.25.014300

Document Version
Publisher's PDF, also known as Version of record

Citation for published version (Harvard):
Guo, Q, Schlickriede, C, Wang, D, Liu, H, Xiang, Y, Zentgraf, T & Zhang, S 2017, 'Manipulation of vector beam polarization with geometric metasurfaces', Optics Express, vol. 25, no. 13, pp. 14300-14307. https://doi.org/10.1364/OE.25.014300

Research Article | Vol. 25, No. 13 | 26 Jun 2017 | OPTICS EXPRESS 14300
Optics EXPRESS

Manipulation of vector beam polarization with geometric metasurfaces

Qinghua Guo,[1,2,5] Christian Schlickriede,[3,5] Dongyang Wang,[2,4,5] Hongchao Liu,[2] Yuanjiang Xiang,[1,6] Thomas Zentgraf,[3,7] and Shuang Zhang[2,*]

[1]*SZU-NUS Collaborative Innovation Centre for Optoelectronic Science & Technology, Key Laboratory of Optoelectronic Devices and Systems of Ministry of Education and Guangdong Province, College of Optoelectronic Engineering, Shenzhen University, Shenzhen 518060, China*
[2]*School of Physics & Astronomy, University of Birmingham, Birmingham, B15 2TT, UK*
[3]*Department of Physics, University of Paderborn, Warburger Straße 100, Paderborn D-33098, Germany*
[4]*Center for Terahertz Waves and College of Precision Instrument and Optoelectronics Engineering, Tianjin University, Tianjin 300072, China*
[5]*These authors contributed equally to this work*
[6]*xiangyuanjiang@126.com*
[7]*thomas.zentgraf@uni-paderborn.de*
[*]*s.zhang@bham.ac.uk*

Abstract: Describing a class of beams with space-variant polarization, vector beams find many applications in both classical and quantum optics. However, simultaneous manipulation of its space-dependent polarization states is still a challenge with a single optical element. Here we demonstrate polarization modulation of a vector field by employing a plasmonic metasurface exhibiting strong and controllable optical activity. By changing the lateral phase shift between two reflective metasurface supercells, the rotation angle of a linear polarized light can be continuously tuned from zero to π with a high efficiency. As the optical activity of our metasurface devices only depends on geometrical phase, the metasurfaces can simultaneously modulate the rotation angle of a vector beam regardless of its space-variant polarization distribution. Our work provides a high efficient method in manipulating the polarization state of vector beams, especially with metasurface in a compact space, which presents great potential in research fields involving vector beams.

OCIS codes: (160.3918) Metamaterials; (050.6624) Subwavelength structures.

References and links

1. Q. Zhan, "Trapping metallic Rayleigh particles with radial polarization," Opt. Express **12**(15), 3377–3382 (2004).
2. X. L. Wang, J. Chen, Y. Li, J. Ding, C. S. Guo, and H. T. Wang, "Optical orbital angular momentum from the curl of polarization," Phys. Rev. Lett. **105**(25), 253602 (2010).
3. A. F. Abouraddy and K. C. Toussaint, Jr., "Three-dimensional polarization control in microscopy," Phys. Rev. Lett. **96**(15), 153901 (2006).
4. G. Bautista, M. J. Huttunen, J. Mäkitalo, J. M. Kontio, J. Simonen, and M. Kauranen, "Second-harmonic generation imaging of metal nano-objects with cylindrical vector beams," Nano Lett. **12**(6), 3207–3212 (2012).
5. G. Bautista, M. J. Huttunen, J. M. Kontio, J. Simonen, and M. Kauranen, "Third- and second-harmonic generation microscopy of individual metal nanocones using cylindrical vector beams," Opt. Express **21**(19), 21918–21923 (2013).
6. M. P. Backlund, A. Arbabi, P. N. Petrov, E. Arbabi, S. Saurabh, A. Faraon, and W. E. Moerner, "Removing orientation-induced localization biases in single-molecule microscopy using a broadband metasurface mask," Nat. Photonics **10**(7), 459–462 (2016).
7. C. Hnatovsky, V. Shvedov, W. Krolikowski, and A. Rode, "Revealing local field structure of focused ultrashort pulses," Phys. Rev. Lett. **106**(12), 123901 (2011).
8. C. Gabriel, A. Aiello, W. Zhong, T. G. Euser, N. Y. Joly, P. Banzer, M. Förtsch, D. Elser, U. L. Andersen, Ch. Marquardt, P. St. J. Russell, and G. Leuchs, "Entangling different degrees of freedom by quadrature squeezing cylindrically polarized modes," Phys. Rev. Lett. **106**(6), 060502 (2011).

#295449 https://doi.org/10.1364/OE.25.014300
Journal © 2017 Received 8 May 2017; revised 24 May 2017; accepted 24 May 2017; published 13 Jun 2017

Optics EXPRESS

9. V. Parigi, V. D'Ambrosio, C. Arnold, L. Marrucci, F. Sciarrino, and J. Laurat, "Storage and retrieval of vector beams of light in a multiple-degree-of-freedom quantum memory," Nat. Commun. **6**, 7706 (2015).
10. Q. Zhan and J. Leger, "Focus shaping using cylindrical vector beams," Opt. Express **10**(7), 324–331 (2002).
11. Z. Man, L. Du, C. Min, Y. Zhang, C. Zhang, S. Zhu, H. Paul Urbach, and X. C. Yuan, "Dynamic plasmonic beam shaping by vector beams with arbitrary locally linear polarization states," Appl. Phys. Lett. **105**(1), 011110 (2014).
12. A. V. Kildishev, A. Boltasseva, and V. M. Shalaev, "Planar photonics with metasurfaces," Science **339**(6125), 1232009 (2013).
13. N. Yu and F. Capasso, "Flat optics with designer metasurfaces," Nat. Mater. **13**(2), 139–150 (2014).
14. N. Meinzer, W. L. Barnes, and I. R. Hooper, "Plasmonic meta-atoms and metasurfaces," Nat. Photonics **8**(12), 889–898 (2014).
15. A. E. Minovich, A. E. Miroshnichenko, A. Y. Bykov, T. V. Murzina, D. N. Neshev, and Y. S. Kivshar, "Functional and nonlinear optical metasurfaces," Laser Photonics Rev. **9**(2), 195–213 (2015).
16. X. Yin, Z. Ye, J. Rho, Y. Wang, and X. Zhang, "Photonic spin Hall effect at metasurfaces," Science **339**(6126), 1405–1407 (2013).
17. X. Ni, Z. J. Wong, M. Mrejen, Y. Wang, and X. Zhang, "An ultrathin invisibility skin cloak for visible light," Science **349**(6254), 1310–1314 (2015).
18. K. A. Tetz, L. Pang, and Y. Fainman, "High-resolution surface plasmon resonance sensor based on linewidth-optimized nanohole array transmittance," Opt. Lett. **31**(10), 1528–1530 (2006).
19. Y. Shen, J. Zhou, T. Liu, Y. Tao, R. Jiang, M. Liu, G. Xiao, J. Zhu, Z. K. Zhou, X. Wang, C. Jin, and J. Wang, "Plasmonic gold mushroom arrays with refractive index sensing figures of merit approaching the theoretical limit," Nat. Commun. **4**, 2381 (2013).
20. W. Li, Z. J. Coppens, L. V. Besteiro, W. Wang, A. O. Govorov, and J. Valentine, "Circularly polarized light detection with hot electrons in chiral plasmonic metamaterials," Nat. Commun. **6**, 8379 (2015).
21. S. Jiang, X. Xiong, Y. Hu, Y. Hu, G. Ma, R. Peng, C. Sun, and M. Wang, "Controlling the Polarization State of Light with a Dispersion-Free Metastructure," Phys. Rev. X **4**(2), 021026 (2014).
22. F. Ding, Z. Wang, S. He, V. M. Shalaev, and A. V. Kildishev, "Broadband high-efficiency half-wave plate: a supercell-based plasmonic metasurface approach," ACS Nano **9**(4), 4111–4119 (2015).
23. Y. Zhao and A. Alù, "Tailoring the dispersion of plasmonic nanorods to realize broadband optical meta-waveplates," Nano Lett. **13**(3), 1086–1091 (2013).
24. B. Yang, W. M. Ye, X. D. Yuan, Z. H. Zhu, and C. Zeng, "Design of ultrathin plasmonic quarter-wave plate based on period coupling," Opt. Lett. **38**(5), 679–681 (2013).
25. Z. Wang, H. Jia, K. Yao, W. Cai, H. Chen, and Y. Liu, "Circular dichroism metamirrors with near-perfect extinction," ACS Photonics **3**(11), 2096–2101 (2016).
26. M. Kuwata-Gonokami, N. Saito, Y. Ino, M. Kauranen, K. Jefimovs, T. Vallius, J. Turunen, and Y. Svirko, "Giant optical activity in quasi-two-dimensional planar nanostructures," Phys. Rev. Lett. **95**(22), 227401 (2005).
27. V. A. Fedotov, P. L. Mladyonov, S. L. Prosvirnin, A. V. Rogacheva, Y. Chen, and N. I. Zheludev, "Asymmetric propagation of electromagnetic waves through a planar chiral structure," Phys. Rev. Lett. **97**(16), 167401 (2006).
28. A. V. Rogacheva, V. A. Fedotov, A. S. Schwanecke, and N. I. Zheludev, "Giant gyrotropy due to electromagnetic-field coupling in a bilayered chiral structure," Phys. Rev. Lett. **97**(17), 177401 (2006).
29. M. Decker, M. W. Klein, M. Wegener, and S. Linden, "Circular dichroism of planar chiral magnetic metamaterials," Opt. Lett. **32**(7), 856–858 (2007).
30. N. Yu, P. Genevet, M. A. Kats, F. Aieta, J. P. Tetienne, F. Capasso, and Z. Gaburro, "Light Propagation with Phase Discontinuities: Generalized Laws of Reflection and Refraction," Science **334**(6054), 333–337 (2011).
31. X. Ni, N. K. Emani, A. V. Kildishev, A. Boltasseva, and V. M. Shalaev, "Broadband light bending with plasmonic nanoantennas," Science **335**(6067), 427 (2012).
32. L. Huang, X. Chen, H. Mühlenbernd, G. Li, B. Bai, Q. Tan, G. Jin, T. Zentgraf, and S. Zhang, "Dispersionless phase discontinuities for controlling light propagation," Nano Lett. **12**(11), 5750–5755 (2012).
33. S. Sun, K. Y. Yang, C.-M. Wang, T.-K. Juan, W. T. Chen, C. Y. Liao, Q. He, S. Xiao, W.-T. Kung, G.-Y. Guo, L. Zhou, and D. P. Tsai, "High-efficiency broadband anomalous reflection by gradient meta-surfaces," Nano Lett. **12**(12), 6223–6229 (2012).
34. C. Pfeiffer and A. Grbic, "Metamaterial Huygens' surfaces: tailoring wave fronts with reflectionless sheets," Phys. Rev. Lett. **110**(19), 197401 (2013).
35. C. H. Chu, M. L. Tseng, J. Chen, P. C. Wu, Y.-H. Chen, H.-C. Wang, T.-Y. Chen, W. T. Hsieh, H. J. Wu, G. Sun, and D. P. Tsai, "Active dielectric metasurface based on phase-change medium," Laser Photonics Rev. **10**(6), 986–994 (2016).
36. S. Sun, Q. He, S. Xiao, Q. Xu, X. Li, and L. Zhou, "Gradient-index meta-surfaces as a bridge linking propagating waves and surface waves," Nat. Mater. **11**(5), 426–431 (2012).
37. J. Lin, J. P. Mueller, Q. Wang, G. Yuan, N. Antoniou, X. C. Yuan, and F. Capasso, "Polarization-controlled tunable directional coupling of surface plasmon polaritons," Science **340**(6130), 331–334 (2013).
38. L. Huang, X. Chen, B. Bai, Q. Tan, G. Jin, T. Zentgraf, and S. Zhang, "Helicity dependent directional surface plasmon polariton excitation using a metasurface with interfacial phase discontinuity," Light Sci. Appl. **2**(3), e70 (2013).
39. D. Lin, P. Fan, E. Hasman, and M. L. Brongersma, "Dielectric gradient metasurface optical elements," Science **345**(6194), 298–302 (2014).

Optics EXPRESS

40. X. Chen, L. Huang, H. Mühlenbernd, G. Li, B. Bai, Q. Tan, G. Jin, C.-W. Qiu, S. Zhang, and T. Zentgraf, "Dual-polarity plasmonic metalens for visible light," Nat. Commun. **3**, 1198 (2012).
41. F. Aieta, M. A. Kats, P. Genevet, and F. Capasso, "Multiwavelength achromatic metasurfaces by dispersive phase compensation," Science **347**(6228), 1342–1345 (2015).
42. F. Qin, K. Huang, J. Wu, J. Jiao, X. Luo, C. Qiu, and M. Hong, "Shaping a subwavelength needle with ultra-long focal length by focusing azimuthally polarized light," Sci. Rep. **5**(1), 9977 (2015).
43. J. Lin, P. Genevet, M. A. Kats, N. Antoniou, and F. Capasso, "Nanostructured holograms for broadband manipulation of vector beams," Nano Lett. **13**(9), 4269–4274 (2013).
44. X. Ni, A. V. Kildishev, and V. M. Shalaev, "Metasurface holograms for visible light," Nat. Commun. **4**, 2807 (2013).
45. L. Huang, X. Chen, H. Mühlenbernd, H. Zhang, S. Chen, B. Bai, Q. Tan, G. Jin, K. W. Cheah, C. W. Qiu, J. Li, T. Zentgraf, and S. Zhang, "Three-dimensional optical holography using a plasmonic metasurface," Nat. Commun. **4**, 2808 (2013).
46. W. T. Chen, K. Y. Yang, C. M. Wang, Y. W. Huang, G. Sun, I. D. Chiang, C. Y. Liao, W. L. Hsu, H. T. Lin, S. Sun, L. Zhou, A. Q. Liu, and D. P. Tsai, "High-efficiency broadband meta-hologram with polarization-controlled dual images," Nano Lett. **14**(1), 225–230 (2014).
47. G. Zheng, H. Mühlenbernd, M. Kenney, G. Li, T. Zentgraf, and S. Zhang, "Metasurface holograms reaching 80% efficiency," Nat. Nanotechnol. **10**(4), 308–312 (2015).
48. K. Huang, Z. Dong, S. Mei, L. Zhang, Y. Liu, H. Liu, H. Zhu, J. Teng, B. Luk'yanchuk, J. K. W. Yang, and C. Qiu, "Silicon Multi-Meta-holograms for the Broadband Visible Light," Laser Photonics Rev. **10**(3), 500–509 (2016).
49. M. Q. Mehmood, S. Mei, S. Hussain, K. Huang, S. Y. Siew, L. Zhang, T. Zhang, X. Ling, H. Liu, J. Teng, A. Danner, S. Zhang, and C.-W. Qiu, "Visible-Frequency Metasurface for Structuring and Spatially Multiplexing Optical Vortices," Adv. Mater. **28**(13), 2533–2539 (2016).
50. F. Y. Yue, D. D. Wen, J. T. Xin, B. D. Gerardot, J. Li, and X. Z. Chen, "Structured beam generation with a single plasmonic metasurface," ACS Photonics **3**(9), 1558–1563 (2016).
51. A. Shaltout, J. Liu, V. M. Shalaev, and A. V. Kildishev, "Optically active metasurface with non-chiral plasmonic nanoantennas," Nano Lett. **14**(8), 4426–4431 (2014).
52. W. Ye, Q. Guo, Y. Xiang, D. Fan, and S. Zhang, "Phenomenological modeling of geometric metasurfaces," Opt. Express **24**(7), 7120–7132 (2016).
53. Q. Zhan, "Cylindrical vector beams: from mathematical concepts to applications," Adv. Opt. Photonics **1**(1), 1–57 (2009).

1. Introduction

The capability of manipulating the local polarization states of light is of vital importance in both fundamental studies and applications. Vector beams, which have a space-variant polarization in the transverse plane, have attracted much research attention in recent years, due to their intriguing and wide applications, including optical trapping [1,2], optical microscopy [3–6], optical micro-fabrication [7] and quantum information processing [8,9]. It is very important to realize the manipulation of vector beams polarization, especially in integrated systems. However, by utilizing combined optical elements [10,11], conventional methods to convert the polarization states of a vector beam usually suffer from complex and bulky configurations, which is not compatible with the primary trend of integration and miniaturization in photonics.

In recent years, optical metasurfaces have gained increasing attention due to their remarkable abilities in light manipulation, versatility, ease of on-chip fabrication, and integration owing to their planar profiles [12–15]. Many exotic phenomena and useful flat optical devices have been demonstrated with metasurfaces such as Photonic Spin Hall Effect, cloaking, sensors, and control of polarization states [16–25]. In particular, it has been shown that with proper metasurface design the polarization angle of linear polarized light can be rotated in the same way as the optical activity (OA) effect [26–29]. However, most of the OA effects from plasmonic metasurface devices experience a strong dispersion due to resonant characteristics of the plasmon modes. In addition, most of the designs depend on the polarization of input light. All these present challenge in the polarization manipulation of a vector beam.

In contrast, geometric metasurfaces that can introduce robust and dispersionless phase jumps along the light path to manipulate phase, amplitude, and polarization of light over subwavelength propagation distances have shown great advantages in realizing integrated

Optics EXPRESS

optical devices, such as anomalous reflection/refraction [30–35], directional couplers for surface plasmon polaritons [36–38], planar focusing lenses [39–42], high-resolution optical holograms [43–48] and beam structuring [49,50]. In geometric metasurfaces, giant OA with non-chiral plasmonic nano-antennas based on the phase shift between left and right circularly polarized components can overcome the strong dependency of incident polarization direction and makes the tunable chiral effects in integrated optics possible [51]. In this work, we employ a reflective metasurface to arbitrarily manipulate the polarization state of vector beams. The vector fields rotation angle could be easily modulated by introducing different phase shift between two supercells of the metasurface. Four different samples are designed and fabricated to show the modulation ability of the metasurface with superior robustness and efficiency.

2. Theory

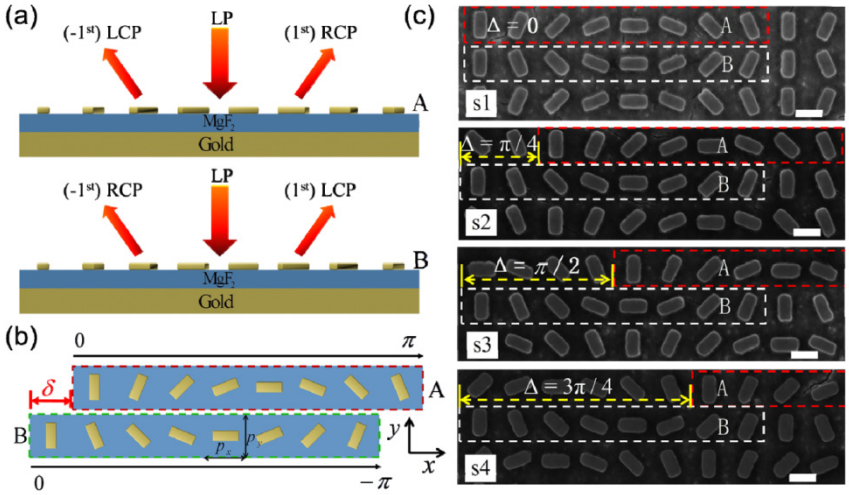

Fig. 1. Optical activity obtained by metasurfaces. (a) For linearly polarized light reflected by the metasurface A/B, right/left- and left/right-handed circularly polarized components are diffracted into the (± 1) first diffraction orders, respectively. (b) Each unit A or B contains eight gold nanorods with variable rotation angle from zero to π or from $-\pi$ to zero. The reflected linear polarization direction in the first diffraction orders can be realized by introducing a geometric phase shiftΔbetween the units A and B. (c) Scanning electron microscopy images of the four metasurface samples s1, s2, s3 and s4, which are fabricated by electron beam lithography technique (scale bar: 200 nm). The geometric phase shift between A and B is zero for s1, $\pi/4$ for s2, $\pi/2$ for s3 and $3\pi/4$ for s4.

The simplest form of geometric metasurface consists of an array of plasmonic antennas with a linear gradient in their orientation angle along a certain direction. For a circularly polarized beam incident onto the metasurface, the scattering of light with opposite spins acquires a spin-dependent geometric phase of twice the orientation angle of the antenna. As such, the gradient in orientation angle translates into a gradient in phase, leading to diffraction of light into a spin-dependent diffraction order.

Here we closely follow the metasurface design in Reference [51]. We design and fabricate reflective metasurfaces that simultaneously generate two spin eigenstates with pre-designed phase difference between them to modulate the vector beams with high efficiency. As shown in Fig. 1(a), the plasmonic metasurface for realizing OA consists of periodic A and B sub-units arranged alternately along y direction. In sub-units A and B, each unit has total eight gold nanorods with a $\pi/8$ rotated angle difference in two neighboring nanorods along x-axis. And the rotation directions of eight nanorods in A and B are opposite to each other. If linearly polarized light with polarization direction parallel to the x-y plane is normally incident onto the metasurface composed with only unit A, the anomalous right circularly polarized light

Optics EXPRESS

(RCP) and left circularly polarized light (LCP) are diffracted to ± 1st orders [32,52]. Inversely, RCP and LCP polarized light diffract along the ± 1st orders after passing through a metasurface composed with only unit B. Hence in order to restore a linear polarization in the diffracted orders, both unit A and B are employed to construct the metasurface. At both diffraction orders (± 1st), linearly polarized light is obtained with the same polarization if the geometric distribution of sub-unit A and B is aligned.

As shown in Fig. 1(b), if we introduce a spatial shift δ along *x*-axis direction between sub-unit A and B, a corresponding phase shift of $2\Delta = 2\pi\delta / p$ is added between the LCP and RCP diffracted in the same direction, where p is the length of the sub-unit. Let the polarization of incident light has a azimuth angle of α_0 relative to *x*-axis, its polarization direction can be defined by Jones matrix: $\frac{\sqrt{2}}{4}\begin{pmatrix}1\\ i\end{pmatrix}e^{-i\alpha_0} + \frac{\sqrt{2}}{4}\begin{pmatrix}1\\ -i\end{pmatrix}e^{i\alpha_0}$, where $\begin{pmatrix}1\\ i\end{pmatrix}$ and $\begin{pmatrix}1\\ -i\end{pmatrix}$ are the two bases for LCP and RCP, respectively. After introducing a phase shift Δ between the A and B metasurface sub-units, the electric fields polarization of diffracted light at ± 1 orders could be then described by the following equations:

$$E_{+1} = \frac{\sqrt{2}}{4}\begin{pmatrix}1\\ -i\end{pmatrix}e^{i\alpha_0} + \frac{\sqrt{2}}{4}\begin{pmatrix}1\\ i\end{pmatrix}e^{-2i\Delta}e^{-i\alpha_0} = \frac{\sqrt{2}}{2}e^{-i\Delta}\begin{pmatrix}\cos(\alpha_0+\Delta)\\ \sin(\alpha_0+\Delta)\end{pmatrix} \quad (1)$$

$$E_{-1} = \frac{\sqrt{2}}{4}\begin{pmatrix}1\\ i\end{pmatrix}e^{-i\alpha_0} + \frac{\sqrt{2}}{4}\begin{pmatrix}1\\ -i\end{pmatrix}e^{2i\Delta}e^{i\alpha_0} = \frac{\sqrt{2}}{2}e^{i\Delta}\begin{pmatrix}\cos(\alpha_0+\Delta)\\ \sin(\alpha_0+\Delta)\end{pmatrix} \quad (2)$$

From the equations, we can see that the phase shift between the LCP and RCP leads to a $180^0 \cdot \Delta / \pi$ polarization rotation of the output. So the lateral phase shift Δ between the two metasurface units determines the rotation angle of linear polarized light at the two diffraction orders. More interestingly, when the polarization direction of light is continuously rotated in the *x*-*y* plane, the net rotation angle is kept the same, which means our design has no dispersion and is not limited by initial polarization directions, thus providing a potential way to modulate the vector beams in integrated system.

3. Experimental results

The metasurface with sub-units A and B consists of three layers with a metal-dielectric-metal sandwich configuration. The bottom gold metal layer and middle MgF_2 dielectric layer have thicknesses of 130 nm and 90 nm, respectively. The top layer consists of gold nanorods with length L = 200 nm, width W = 80 nm and height H = 30 nm. The cells are arranged with periods P_x = 300 nm and P_y = 300 nm, as labeled in Fig. 1(b). The dimension of a metasurface sample is 300 × 300 μm^2. Figure 1(c) shows the SEM images of four metasurface samples s1, s2, s3 and s4, in which the lateral phase shift Δ between A and B units are zero, π/4, π/2 and 3π/4, respectively. The OA effects from the composite metasurfaces are measured by using a supercontinuum laser source (Fianium SP 400C-PP). After passing through a linear polarizer, the linearly polarized light is focused onto the plasmonic metasurface by a convex lens with focal length of 75 mm. The first order diffraction at angle of $\pm\arcsin(\lambda_0 / p)$ from the gold metasurface is analyzed by the second linear polarizer and an InGaAs Infrared power meter. The working wavelength in this work is tuned fromλ_0 = 600 nm to 1100 nm at a step of 50 nm.

Figure 2(a) shows the polarization rotation of the reflected beam by four metasurface devices versus the wavelength of incident light. The polarization angle of the incident light is set along *x*-axis. For the two diffraction orders, the rotation angles of linear polarization from all four samples show almost no dispersion in the measuring wavelength range (600 nm to 1100 nm). The reflected rotation angle only depends on the lateral spatial shift between the A

Optics EXPRESS

and B units, which agrees with the previous theoretical analysis. It is worthy to mention that the polarization direction at both of ± 1 orders rotates along clockwise direction. This unintuitive result is actually reasonable as the metasurface units break the mirror symmetry and thus the rotation angle at the two first orders do not need to be opposite. Because the polarization rotation angle is determined by the phase delay between LCP and RCP eigenstates, the phase shift is only caused by the geometric dislocation of the two subunits. It is expected that the net rotation angle Δis a constant for a variable polarization angle of the incident light. This is also experimentally verified in Fig. 2(b), which shows the linear relation between input and output polarization angles. The net rotation angle remains 0, 45, 90, 135 degree for the four samples, while the input polarization angle in the *x*-*y* plane is continuously rotated. This independence to the initial polarization angle is the key to realize the vector beam modulator, which is difficult for most plasmonic and metamaterial devices that have strong plasmon resonances for particular polarization states and thus OA effect in those devices are usually sensitive to the direction of input polarization.

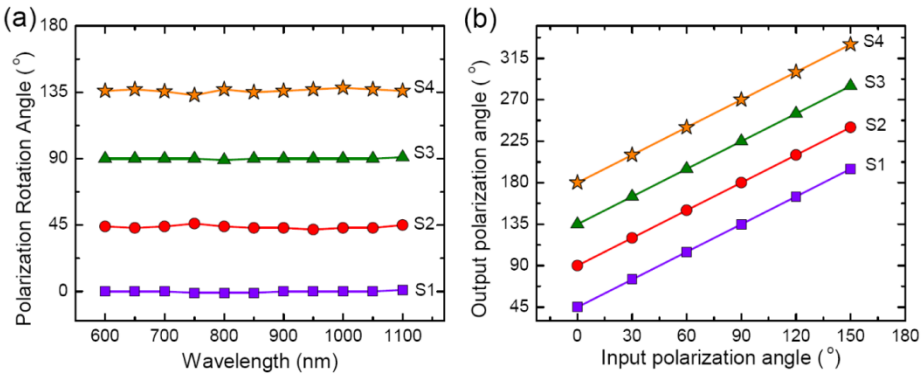

Fig. 2. Experimental results of the optical activity effect. (a) Dispersionless polarization rotation angles for the four metasurface devices at the + 1st diffraction orders. (b) Linear relationship between initial polarization angle and that of the + 1st order diffraction from the metasurfaces.

In order to verify the manipulation of the polarization state of the vector beams with the metasurfaces, we use a vector beam with $m = 1$ as the incident light [53]. The polarization distribution of the vector beam is shown in Fig. 3(a), which is verified by the fan-shaped intensity pattern after passing through an analyzer with direction indicated by the double-headed arrow in Fig. 3(f). The vector beam is then incident onto the four metasurface samples and the corresponding intensity distributions of the reflected fields are measured. The intensity distributions show no difference after being reflected by the four samples as shown in Figs. 3(b)-3(e), which exhibit the same donut shape. In order to observe the rotation of polarization, we measure the intensity distribution of the reflected beams after the same analyzer whose direction is indicated by the double-headed arrow in Fig. 3(f). Figures 3(g)-3(j) show the fan-shaped pattern with different direction corresponding to four different samples, which clearly verify that the vector beams have the field vector distribution as indicated by arrows in Figs. 3(b)-3(e) after reflected by the metasurfaces. We therefore successfully realize the vector beam polarization rotation with a single metasurface.

Optics EXPRESS

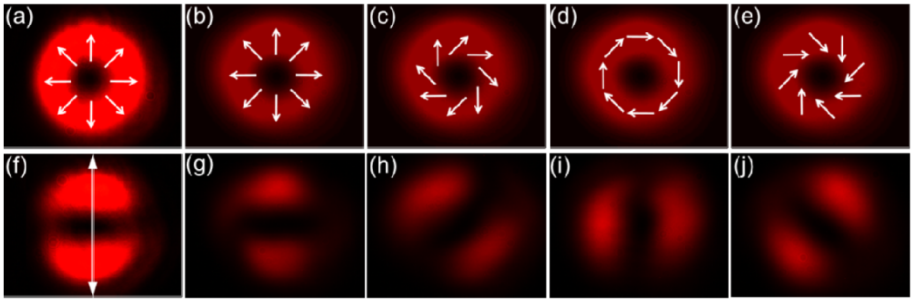

Fig. 3. Experimental results of the vector beam modulation. (a) The intensity distributions of a radially polarized which incident on the samples, with the white arrows representing the polarization distribution of the beam pattern. (b-e) Intensity and field vector distribution of the vector beam reflected by sample 1, 2, 3 and 4 respectively, without analyzer. (f-j) When an analyzer is used, the fan-like extinction pattern appears in intensity distribution, owing to the cylindrical symmetry polarization distribution in the beam cross section, which shows the polarization distribution of the vector beams.

We further determine the conversion efficiency of our reflected metasurfaces. Figure 4 shows the conversion efficiency of samples s2 and s3 with incident wavelength ranging from 700 to 1000 nm. Because our metasurface has two subunits which are arranged in an alternating order, the efficiency is not as high as the case in reference [47], where single function nanorods are empolyed. Nevertheless, the efficiency of our reflective metasurface is measured to be 27% for each diffraction order, which is much higher than the transmissive type metasurfaces [51] and may be sufficient for most practical applications.

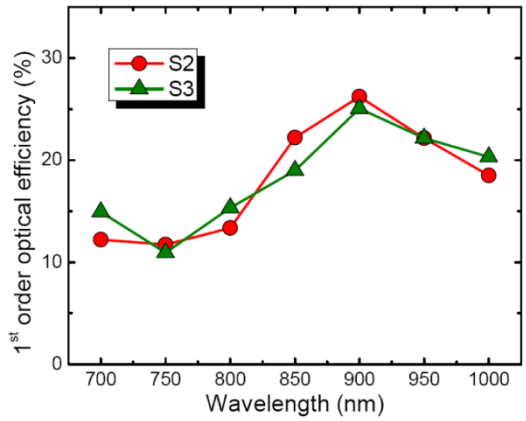

Fig. 4. Experimentally obtained optical vector beam conversion efficiency of the first diffracted order corresponding to sample s2 and s3 with different incident wavelength.

4. Conclusions

In conclusion, we demonstrate a dispersionless, high-efficiency and broadband vector beam modulator by using ultrathin reflective metasurfaces consisting of specific arrangement of plasmonic nanorods. The rotation angle of each linear polarization over the transverse profile of the vector beam can be tuned simultaneously from zero to π by introducing a lateral shift between two metasurface sub-units. The stability and high conversion efficiency (up to 27% for each diffraction order) of our reflective metasurface shows a great potential for applications involving vector beams, such as microscopy imaging, optical trapping and quantum communications.

Optics EXPRESS

Funding

Natural National Science Foundation of China (NSFC) (11604216, 61490713, 61505111); China Postdoctoral Science Foundation (2016M600667); Deutsche Forschungsgemeinschaft DFG (ZE953/7-1, GRK 1464/2 A08); ERC Consolidator Grant (TOPOLOGICAL); Royal Society Wolfson Research Merit Award.